

---

# Differential dynamics of splicing factor SC35 during the cell cycle

KAUSHLENDRA TRIPATHI and VEENA K PARNAIK\*

Centre for Cellular and Molecular Biology, Hyderabad 500 007, India

\*Corresponding author (Fax, +91-40-27160591; Email, veenap@ccmb.res.in)

Pre-mRNA splicing factors are enriched in nuclear domains termed interchromatin granule clusters or nuclear speckles. During mitosis, nuclear speckles are disassembled by metaphase and reassembled in telophase in structures termed mitotic interchromatin granules (MIGs). We analysed the dynamics of the splicing factor SC35 in interphase and mitotic cells. In HeLa cells expressing green fluorescent protein (GFP)-SC35, this was localized in speckles during interphase and dispersed in metaphase. In telophase, GFP-SC35 was highly enriched within telophase nuclei and also detected in MIGs. Fluorescence recovery after photobleaching (FRAP) experiments revealed that the mobility of GFP-SC35 was distinct in different mitotic compartments. Interestingly, the mobility of GFP-SC35 was 3-fold higher in the cytoplasm of metaphase cells compared with interphase speckles, the nucleoplasm or MIGs. Treatment of cells with inhibitors of cyclin-dependent kinases (cdks) caused changes in the organization of nuclear compartments such as nuclear speckles and nucleoli, with corresponding changes in the mobility of GFP-SC35 and GFP-fibrillarin. Our results suggest that the dynamics of SC35 are significantly influenced by the organization of the compartment in which it is localized during the cell cycle.

[Tripathi K and Parnaik V K 2008 Differential dynamics of splicing factor SC35 during the cell cycle; *J. Biosci.* **33** 345–354]

---

## 1. Introduction

The nucleus is compartmentalized into specific protein-rich domains such as the nucleolus, nuclear speckles or splicing factor compartments, Cajal bodies and promyelocytic leukaemia bodies (reviewed by Lamond and Earnshaw 1998; Spector 2003). In mammalian cells, pre-mRNA splicing factors are enriched in 20–50 nuclear speckles that correspond to interchromatin granule clusters (IGCs) at the electron microscopic level, and are also distributed in the nucleoplasm at the sites of transcription on perichromatin fibrils (reviewed by Fakan and Puvion 1980; Spector

1993; Fakan 1994; Lamond and Spector 2003). The major constituents of IGCs are factors involved in RNA processing such as small nuclear ribonucleoproteins (snRNPs) and arginine–serine-rich (RS) splicing factors in mammalian cells (Mintz *et al* 1999). Nuclear speckles are dynamic structures that are involved in the spatial coordination of transcription and splicing (Misteli and Spector 1999; Sacco-Bubulya and Spector 2002). Upon gene activation, splicing factors are recruited to transcription sites (Misteli *et al* 1997) and conversely coalesce to form enlarged foci in the presence of transcriptional inhibitors (Carmo-Fonseca *et al* 1992; Misteli *et al* 1997). The interphase dynamics of speckles

**Keywords.** Cell cycle dynamics; FRAP analysis; mitotic interchromatin granules; splicing factor SC35

Abbreviations used: ASF, alternate splicing factor; cdk, cyclin-dependent kinase; Clk, Cdc2-like kinase; DAPI, 4',6-diamidino-2-phenylindole; FBS, foetal bovine serum; FITC, fluorescein isothiocyanate; FRAP, fluorescence recovery after photobleaching; GFP, green fluorescent protein; GST, glutathione S-transferase; IGC, interchromatin granule cluster; IPTG, isopropyl- $\beta$ -D-thiogalactopyranoside; mAb, monoclonal antibody; MIG, mitotic interchromatin granule; NAP, NOR-associated patch; NOR, nucleolar organizing region; PBS, phosphate-buffered saline; PVDF, polyvinylidene fluoride; RFI, relative fluorescence intensity; RS, serine-rich; SDS-PAGE, sodium dodecyl sulphate-polyacrylamide gel electrophoresis; snRNP, small nuclear ribonucleoprotein; snoRNA, small nucleolar RNA; SRPK 1, serine/arginine-rich protein kinase 1

is controlled by the phosphorylation of splicing factors at RS domains. RS domains are specifically phosphorylated by a number of kinases such as Cdc2-like kinase (Clk/STY kinase) (Ben-David *et al* 1991; Howell *et al* 1991; Johnson and Smith 1991) and serine/arginine-rich protein kinase 1 (SRPK1) (Gui *et al* 1994), leading to recruitment of splicing factors to the sites of transcription (Misteli *et al* 1998). Overexpression of Clk/STY kinase or SRPK1 causes dispersal of speckles in the nucleoplasm in interphase cells and disrupts the coordination between transcription and splicing (Gui *et al* 1994; Colwill *et al* 1996; Sacco-Bubulya and Spector 2002). Other kinases such as cyclin-dependent kinase (cdk)-9, cyclin T and CrkRS, which are involved in phosphorylation of the C-terminal domain of the largest subunit of RNA polymerase II, are localized in the vicinity of speckles (Herrmann and Mancini 2001; Ko *et al* 2001).

During mitosis, nuclear speckles are disassembled by metaphase and reassembled in telophase in cytoplasmic structures termed mitotic interchromatin granules (MIGs), based on their similarity to IGCs in composition and granular appearance (Reuter *et al* 1985; Verheijen *et al* 1986; Leser *et al* 1989; Spector *et al* 1991; Ferreira *et al* 1994). After formation of the nascent nuclear envelope in telophase, there is sequential nuclear import of RNA polymerase II and transcription factors, followed by entry of pre-mRNA splicing factors; certain splicing factors such as SF2/alternate splicing factor (ASF) and B<sup>+</sup> remain highly enriched in MIGs till late telophase (Prasanth *et al* 2003). Although the dynamics of SF2/ASF in interphase cells has been well documented (Phair and Misteli 2000; Kruhlak *et al* 2000), the dynamics of splicing factors at different stages of mitosis have not been reported.

In the present study, we analysed the localization and dynamics of the splicing factor SC35 in HeLa cells expressing GFP-SC35. The localization of GFP-SC35 in interphase and mitotic cells was determined with respect to markers for nuclear components. The mobility of GFP-SC35 was studied in different compartments in live cells by fluorescence recovery after photobleaching (FRAP) experiments. Cells were treated with inhibitors of cdks to determine their effects on the organization of nuclear compartments such as nuclear speckles and nucleoli, and on the dynamics of GFP-SC35 and the nucleolar protein GFP-fibrillarin. Our results indicate that the dynamics of GFP-SC35 are dependent on the organization of the compartment in which it is localized during the interphase and mitotic phase of the cell cycle.

## 2. Materials and methods

### 2.1 Plasmid constructs

A mouse cDNA for SC35 (provided by Tom Maniatis, Harvard University, Cambridge, MA, USA) was cloned into

*EcoRI/SalI*-digested pEGFP-C2 vector to generate GFP-SC35. A GST-SC35 fusion construct was made by cloning SC35 cDNA into *SmaI/EcoRI*-digested pGEX vector. GFP-SF2/ASF was obtained from Adrian Krainer (CSHL, Cold Spring Harbor, NY, USA) and GFP-fibrillarin was provided by Sui Huang (Northwestern University, Chicago, IL, USA).

### 2.2 Cell culture, DNA transfection and drug treatment

HeLa cells were routinely grown in DMEM supplemented with 10% foetal bovine serum (FBS) at 37°C in a humidified atmosphere containing 5% CO<sub>2</sub>. A HeLa cell line stably expressing GFP-SC35 was generated by electroporation of the GFP-SC35 fusion construct, and maintained in DMEM (low glucose) with 10% FBS and 0.5 mg/ml G418 (Invitrogen, Carlsbad, USA). GFP-fibrillarin or GFP-SF2/ASF constructs were transiently transfected into HeLa cells using Lipofectamine 2000 according to the manufacturer's instructions (Invitrogen). Roscovitine, olomoucine and iso-olomoucine were obtained from Calbiochem (Merck Chemicals, Darmstadt, Germany). Roscovitine was also provided by L Meijer (Station Biologique, Roscoff, France). HeLa cells were treated with 25 µM roscovitine for 1.5 h, or with 250 µM olomoucine or iso-olomoucine for 2 h.

### 2.3 Antibodies and western blot analysis

A mouse monoclonal antibody (mAb) to SC35 was obtained from Sigma Chemical Co. (St Louis, USA). A mouse mAb to emerlin (clone 4G5) was obtained from Novocastra Laboratories (Newcastle-upon-Tyne, UK). Polyclonal antibodies to fibrillarin and GFP were from Santa Cruz Biotechnology (Santa Cruz, USA) and Clontech (Palo Alto, USA), respectively. A mouse mAb to B<sup>+</sup> was a gift from David Spector (CSHL, Cold Spring Harbor, NY, USA). For western blot analysis, cells were harvested, lysed in Laemmli sample buffer, boiled and electrophoresed through sodium dodecyl sulphate (SDS)-10% polyacrylamide gels. Gels were electroblotted onto polyvinylidene fluoride (PVDF) membrane filters and blocked overnight in 5% BLOTTO milk powder in Tris-buffered saline containing 0.1% Tween-20. Filters were incubated with primary antibody for 2 h, followed by peroxidase-conjugated secondary antibody in Tris-buffered saline containing 0.1% Tween-20 for 1 h. Bound antibody was visualized using a chemiluminescence kit from Roche Applied Science (Mannheim, Germany).

### 2.4 Immunofluorescence microscopy

HeLa cells were washed with phosphate-buffered saline (PBS) and then fixed with 4% formaldehyde in PBS for

10 min followed by 0.5% (vol/vol) Triton X-100 for 6 min at room temperature. Cells were then incubated with 0.5% gelatin in PBS for 1 h followed by incubation with primary antibody for 1 h and then Cy3-conjugated second antibody for 1 h at room temperature for single labelling experiments. For double labelling experiments, fixed cells were incubated with the first primary antibody followed by the biotinylated second antibody and avidin-Cy3, and then with the next primary antibody and species/subtype-specific fluorescein isothiocyanate (FITC)-conjugated second antibody. Samples were mounted in Vectashield (Vector Laboratories, Burlingame, USA) containing 1  $\mu\text{g/ml}$  4',6-diamidino-2-phenylindole (DAPI). There was no cross-reactivity of the fluorescent second antibodies in control experiments in which either primary antibody was omitted. Fluorescence microscopy was performed on an LSM510 META confocal microscope. Images were analysed with LSM 510 META software and assembled using Photoshop 6.0.

### 2.5 Live cell microscopy

HeLa cells stably expressing GFP-SC35 (or transiently expressing GFP-fibrillarin or GFP-SF2/ASF) were seeded on a LabTekII chamber slide and grown for 24 h. FRAP experiments were performed on an LSM510 inverted confocal microscope with a 63x/1.4 NA planapochromat water objective lens. A spot 1  $\mu\text{m}$  in radius was bleached for 0.5 s using the 488 nm laser line at 100% laser power, and a series of images were acquired at 1 s intervals immediately after bleaching. Image acquisition was at low laser power, which did not significantly affect fluorescence intensity. Recovery of fluorescence was observed till 100 s. All intensities were background subtracted for calculating the FRAP curves, which represented an average of 12–15 individual cells bleached under identical conditions in at least three independent experiments (cells expressing moderate levels of GFP-SC35 were chosen for analysis). To normalize for loss of fluorescence signal due to the bleach pulse and potential artifactual bleaching of GFP during the imaging scans, recovery intensities were normalized to the total fluorescence signal at each time point. Cells exhibiting a loss of signal of more than 10% during the imaging phase were discarded from analysis. The relative fluorescence intensity (RFI) at each time point was calculated as described by Phair and Misteli (2000), using the equation  $\text{RFI} = (I_t/T_t)/(I_0/T_0)$ , where  $I_0$  and  $I_t$  are the average intensity of the region of interest before and after bleaching at time  $t$ , and  $T_0$  and  $T_t$  are the total intensity in the nucleus before and after bleaching at time  $t$ , respectively. The half-time of fluorescence recovery ( $t/2$ ) was calculated as half the time required for complete recovery of fluorescence after bleaching. Diffusion coefficients were calculated by classical FRAP analysis as described by Axelrod *et al*

(1976). Non-linear curve fitting was carried out using Origin 7.0. In control experiments with formaldehyde-fixed cells, no recovery of fluorescence was observed.

### 2.6 Phosphorylation of recombinant GST-SC35

Recombinant GST-SC35 was expressed in *E. coli* BL21(DE3)-plys(S) by induction with 1 mM isopropyl- $\beta$ -D-thiogalactopyranoside (IPTG) for 3 h at 30°C and purified on glutathione-agarose beads. The purity and quantity of the recombinant protein was determined by analysis on an SDS-polyacrylamide gel electrophoresis (PAGE) gel stained with Coomassie blue. Recombinant GST-SC35 protein was incubated for 30 min at 30°C with 5  $\mu\text{Ci}$  of  $\gamma^{32}\text{P}$ -ATP, 100  $\mu\text{M}$  ATP, 5 mM  $\text{MgCl}_2$ , and 40 U of human Cdk1-cyclin B (New England Biolabs, Beverly, USA) in 20  $\mu\text{l}$  of MEM buffer (100 mM Mes, pH 6.7, 1 mM EGTA, 1 mM  $\text{MgCl}_2$ , 0.1 mM dithiothreitol). A control reaction was performed with kinase storage buffer instead of enzyme. Phosphorylation reactions were stopped with Laemmli buffer supplemented with 10 mM EDTA and samples were processed for SDS-PAGE, followed by analysis of the same gel on a phosphorimager (Molecular Imager FX, Bio-Rad, Hercules, USA).

## 3. Results

### 3.1 Localization of GFP-SC35 in interphase and mitotic cells

Splicing factor compartments comprise ~150 proteins, which include both snRNP proteins and non-snRNP proteins such as SC35 and SF2/ASF (Mintz *et al* 1999). In order to study the dynamics of the splicing factor SC35 during mitosis, we produced a stable HeLa cell line expressing GFP-SC35. The rates of cell division and viability of the parental HeLa cell line and GFP-SC35 stable clone were observed to be similar. Western blot analysis with antibodies to GFP and SC35 indicated that GFP-SC35 migrated at the appropriate mobility and was expressed at low levels compared with endogenous SC35 (figure 1A). The distribution of GFP-SC35 was initially confirmed by fluorescence microscopy with fixed cells (figure 1B). In interphase cells, GFP-SC35 was distributed in a speckled pattern as well as a diffuse nuclear location, as described previously for fluorescent-tagged SC35 (Prasanth *et al* 2003; Politz *et al* 2006). At the onset of mitosis, GFP-SC35 speckles became dispersed in metaphase cells. From metaphase to anaphase, GFP-SC35 was mostly diffusely distributed, though an occasional speckle could be detected. In telophase cells, a substantial fraction of GFP-SC35 was observed within daughter nuclei. The remainder was concentrated in speckles corresponding to MIGs outside the nuclei. The interphase pattern of speckles was restored in

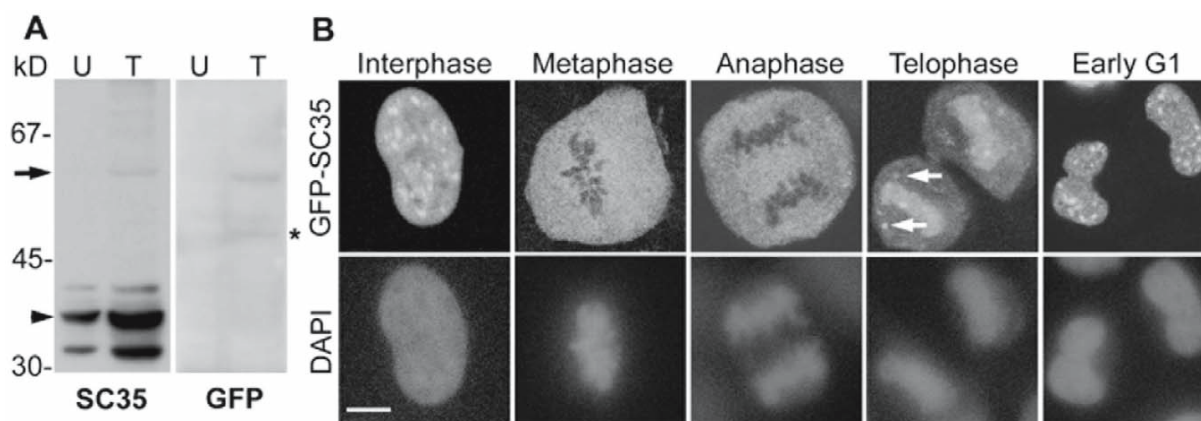


**Figure 1.** Expression of green fluorescent protein (GFP)-SC35 and localization during mitosis. **(A)** Whole cell lysates of untransfected (U) and GFP-SC35-transfected (T) HeLa cells were analysed by western blotting with antibodies to SC35 and GFP. Positions of GFP-SC35 and SC35 (major species) are indicated by an arrow and arrowhead, respectively. This mouse antibody (mAb) to SC35 also labels other differentially phosphorylated forms of SC35. An asterisk points to a non-specific band observed in both untransfected and transfected cell lysates. Molecular mass markers (kD): albumin, 67 kD; ovalbumin, 45 kD; and carbonic anhydrase, 30 kD. **(B)** Mitotic HeLa cells expressing GFP-SC35 were observed at different phases of mitosis by confocal microscopy (optical sections of 0.5  $\mu\text{m}$ ). Arrows indicate GFP-SC35 in speckles outside the telophase nucleus. Bar, 5  $\mu\text{m}$ .

early G1 cells. These experiments indicate that GFP-SC35 is a suitable marker for the physiological functions and distribution of SC35.

The sequence of GFP-SC35 localization at different stages of mitosis was investigated with respect to endogenous nuclear markers. The localization of GFP-SC35 in distinct domains was analysed with a widely-used mAb to SC35, which recognizes a specific hyperphosphorylated form of SC35 present in speckles in interphase cells and in MIGs in mitotic cells, but is absent in metaphase cells and telophase nuclei (Fu and Maniatis 1990). Moreover, this antibody to phosphorylated SC35 would recognize the endogenous protein, which is more abundant in the cells. In interphase cells, GFP-SC35 was localized in nuclear speckles which were stained by the antibody to SC35. However, the antibody did not detect GFP-SC35 in metaphase cells or telophase nuclei, though it stained MIGs in telophase cells, which also harboured GFP-SC35 (figure 2A). The number of MIGs increased from anaphase to telophase and decreased subsequently. SC35 has been earlier detected in a diffuse distribution in metaphase cells (Prasanth *et al* 2003) and within telophase nuclei with an antibody to hypophosphorylated SC35 (Bubulya *et al* 2004). An antibody to the U2 snRNP protein B'' labelled nuclear speckles containing GFP-SC35 in interphase cells (figure 2B). Like other snRNPs, B'' was also localized in Cajal bodies as reported earlier (Prasanth *et al* 2003), but these structures did not contain GFP-SC35. B'' was diffusely distributed in metaphase cells and concentrated in MIGs in telophase cells, where it colocalized with GFP-SC35. The

major fraction of GFP-SC35 and a small amount of B'' were located in telophase nuclei.

Earlier studies have demonstrated that SF2/ASF enters telophase nuclei only after the formation of a functional nuclear envelope (Prasanth *et al* 2003). To confirm that nuclear envelope formation had been initiated when GFP-SC35 was detectable in telophase nuclei, cells were labelled with an antibody to the inner nuclear membrane protein, emerin. As shown in figure 2C, emerin displayed a distinct localization in the nuclear envelope in interphase cells but was dispersed during metaphase when the envelope breaks down. During telophase, emerin was localized at the nascent envelope of telophase nuclei harbouring GFP-SC35. We also determined the distribution of GFP-SC35 with respect to the nucleolar marker fibrillarin (figure 2D). In interphase cells, GFP-SC35 and fibrillarin occupied distinct compartments as expected. During metaphase, both GFP-SC35 and fibrillarin were dispersed. In early telophase nuclei, small foci of fibrillarin were observed, which are likely to be pre-nucleolar bodies (Scheer and Hock 1999), and these domains were surrounded by GFP-SC35 but did not colocalize with it, consistent with the data for SF2/ASF (Bubulya *et al* 2004).

### 3.2 Dynamics of GFP-SC35 in different compartments

To determine the dynamic behaviour of GFP-SC35, FRAP experiments were carried out with HeLa cells stably transfected with GFP-SC35. The mobility of GFP-SC35



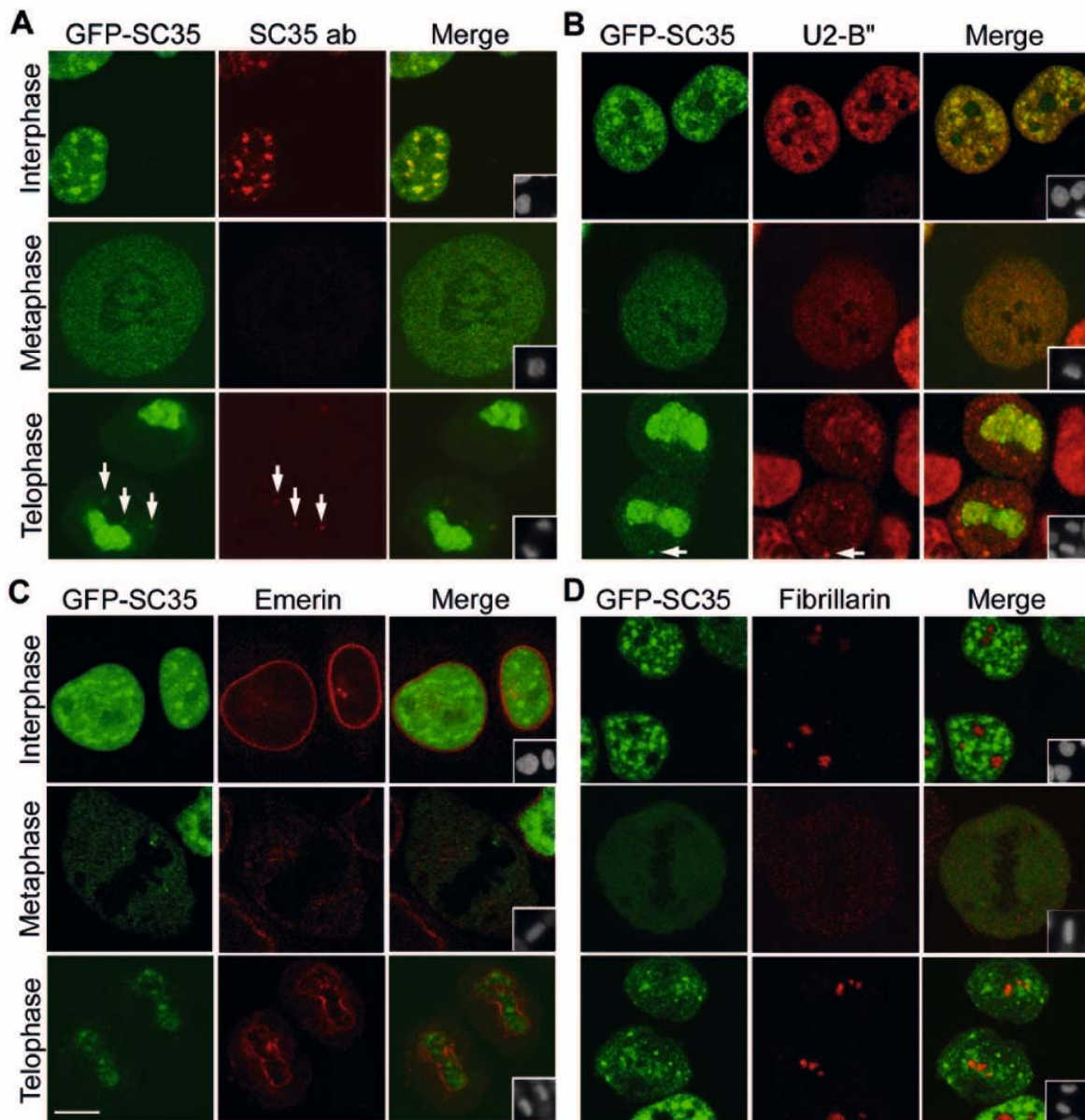


**Figure 2.** Localization of green fluorescent protein (GFP)-SC35 with respect to nuclear markers. Mitotic HeLa cells expressing GFP-SC35 were stained with antibodies to (A) SC35, (B) B'', (C) emerlin and (D) fibrillarin (optical sections of  $0.5 \mu\text{m}$ ). Arrows indicate GFP-SC35 speckles outside telophase nuclei that are colocalized with SC35 and B''. 4',6-diamidino-2-phenylindole (DAPI) staining is shown in the insets. Bar,  $10 \mu\text{m}$ .

was analysed in different compartments in interphase and mitotic cells. A spot with a radius of  $1 \mu\text{m}$  over a speckle or in the nucleoplasm was photobleached. Subsequently, the RFI within the photobleached area was measured. The fluorescence recovery curves were analysed as described (Phair and Misteli 2000). Representative FRAP curves and scanned images of bleached cells are shown in figure 3. Bleaching conditions were optimized for 40–60% bleach as per standard procedures. FRAP analyses revealed that

GFP-SC35 had a half-time of fluorescence recovery ( $t_{1/2}$ ) of  $\sim 2$  s with a diffusion coefficient of  $0.24 \mu\text{m}^2/\text{s}$  in both interphase nuclear speckles and the nucleoplasm, with nearly 90% recovery observed at 30 s (figure 3 and table 1). Similar values were obtained for GFP-SF2/ASF in transiently transfected cells and these values closely correspond to those reported in earlier studies with GFP-SF2/ASF (Phair and Misteli 2000). FRAP data of GFP-SC35 in MIGs in telophase cells were also similar to that of normal interphase

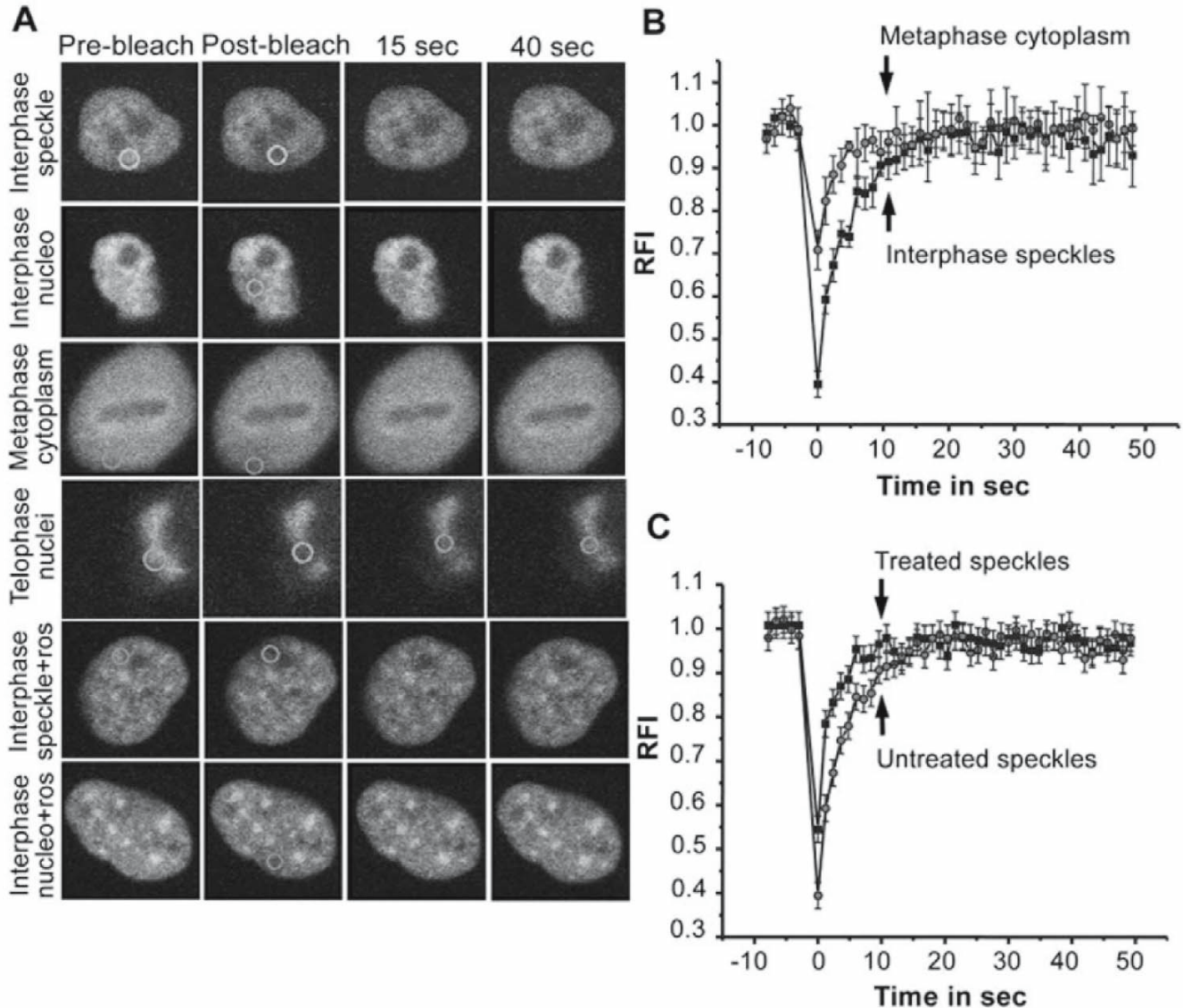


**Figure 3.** Fluorescence recovery after photobleaching (FRAP) analysis of green fluorescent protein (GFP)-SC35. (A) Fluorescence images of FRAP processes of GFP-SC35 for the indicated conditions. Circles indicate areas of bleaching where fluorescence recovery was measured. Two example time points are shown at 15 and 40 s after photobleaching. Bar, 5  $\mu\text{m}$ . (B, C) Graphical presentation of fluorescence recovery as change in relative fluorescence intensity (RFI) over time (post-bleach as zero) for (B) metaphase cytoplasm (circles) and interphase speckles (squares); (C) interphase speckles (circles) and roscovitine-treated interphase speckles (squares). The data for interphase speckles (not treated with roscovitine) are shown in both (B) and (C) for easy comparison.

cells. Interestingly, the recovery of fluorescence from GFP-SC35 distributed diffusely in the cytoplasm of metaphase cells was 3-fold faster than that in speckles or interphase nucleoplasm ( $P < 0.001$ ) and recovery had already occurred while scanning the image of the bleached cell in figure 3A. On the other hand, GFP-SC35 was slightly less mobile in telophase nuclei than in MIGs or speckles and this trend was significant ( $P < 0.001$ ).

We explored the effects of inhibitors of protein phosphorylation by cdks on GFP-SC35 distribution and

dynamics. In interphase cells, when several cdks are normally active, treatment with specific inhibitors of cdks, roscovitine or olomoucine (Meijer *et al* 1997), caused enlargement of GFP-SC35 speckles (figure 4A) and these speckles colocalized with SC35 labelled with a mAb to SC35 (figure 4B). On the other hand, cells treated with isolumoucine as a negative control displayed normal speckles. GFP-SC35 fluorescence was also observed at the periphery of the nucleolus in treated cells, as reported previously for SF2/ASF (Bubulya *et al* 2004). Immunostaining with

**Table 1.** Fluorescence recovery after photobleaching (FRAP) analysis of SC35, SF2/alternate splicing factor (ASF) and fibrillarin

Bleached compartment	Half time ( $t_{1/2}$ ) (s)	Diffusion coefficient ( $\mu\text{m}^2/\text{s}$ )
SC35 in interphase speckles	$2.21 \pm 0.54$	0.237
SC35 in interphase nucleoplasm	$2.10 \pm 0.61$	0.245
SF2/ASF in interphase speckles	$2.27 \pm 0.51$	0.235
SC35 in metaphase cytoplasm	$0.71 \pm 0.08$	0.887
SC35 in telophase MIGs	$2.31 \pm 0.47$	0.235
SC35 in telophase nuclei	$2.97 \pm 0.71$	0.189
SC35 in interphase speckles + roscovitine	$1.70 \pm 0.24$	0.333
SC35 in interphase nucleoplasm + roscovitine	$2.50 \pm 0.51$	0.222
SF2/ASF in interphase speckles + roscovitine	$1.63 \pm 0.22$	0.341
Fibrillarin in nucleolus	$17.5 \pm 3.25$	0.047
Fibrillarin in nucleolus + roscovitine	$7.74 \pm 1.57$	0.088

an antibody to fibrillarin revealed that it was dispersed in treated cells (figure 4B). To determine whether SC35 can be phosphorylated by a cdk, we checked the ability of Cdk1 to phosphorylate SC35 *in vitro*, since purified, active Cdk1–cyclin B1 complex is available commercially. Purified glutathione S-transferase (GST)-tagged SC35 was incubated with Cdk1–cyclin B1 in the presence of  $\gamma^{32}\text{P}$ -ATP. As shown in figure 4, SC35 was phosphorylated by Cdk1–cyclin B1 whereas no phosphorylation was observed in a control reaction with buffer alone. Purified GST was not phosphorylated by Cdk1–cyclin B1 (data not shown). We further confirmed that RNA polymerase II transcription was inhibited by roscovitine and olomoucine (data not shown).

As the speckles enlarged in interphase nuclei after roscovitine or olomoucine treatment, we were interested in analysing the dynamics of GFP-SC35 in these domains. FRAP analysis in roscovitine-treated interphase cells indicated that GFP-SC35 in enlarged speckles became slightly more mobile than in normal interphase speckles with a  $t_{1/2}$  of  $\sim 1.7$  s (figure 3 and table 1). Though the difference was small, the trend was significant ( $P < 0.001$ ). The full fluorescence recovery of GFP-SC35 approached 100%, demonstrating that almost all GFP-SC35 within the bleached region was replaceable. Similar results were obtained with GFP-SF2/ASF in interphase speckles after roscovitine treatment. As we had noted that the nucleolar protein fibrillarin was dispersed in interphase cells after treatment with roscovitine (*see* figure 4C), we also analysed the dynamics of fibrillarin under these conditions. FRAP

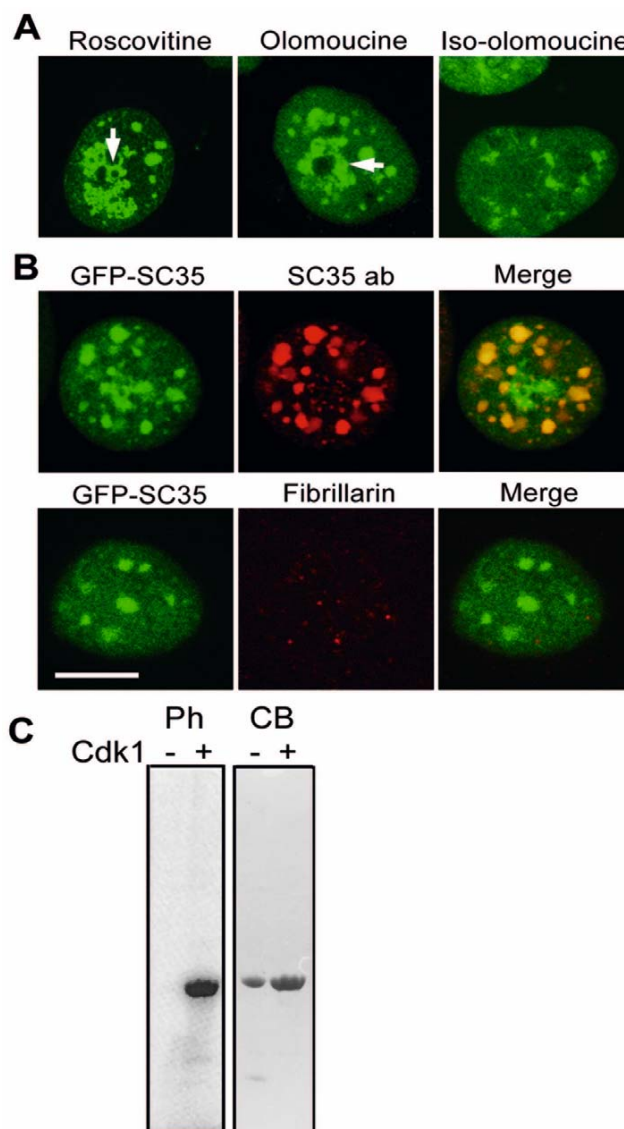


**Figure 4.** Effects of cdk inhibitors on green fluorescent protein (GFP)-SC35 and nuclear markers. (A) HeLa cells expressing GFP-SC35 were treated with roscovitine, olomoucine or iso-olomoucine. (B) HeLa cells expressing GFP-SC35 were treated with roscovitine and stained with antibodies to SC35 or fibrillarin (optical sections of  $0.5 \mu\text{m}$ ). Arrows point to GFP-SC35 localized near the nucleolus after drug treatment. Bar,  $10 \mu\text{m}$ . (C) *In vitro* kinase assays of purified GST-SC35, with or without Cdk1–cyclin B1, showing the phosphorimager analysis of radioactive phosphorylation (Ph) and the Coomassie blue-stained gel (CB).

analysis of GFP-fibrillarin within the nucleolus indicated that its mobility was slow in this compartment ( $D=0.047 \mu\text{m}^2/\text{s}$ ), which was consistent with an earlier report (Phair and Misteli 2000). However, GFP-fibrillarin became 2-fold more mobile after roscovitine treatment ( $P < 0.001$ ), with a reduction in the immobile fraction in the nucleolus, as shown in figure 5 and table 1.



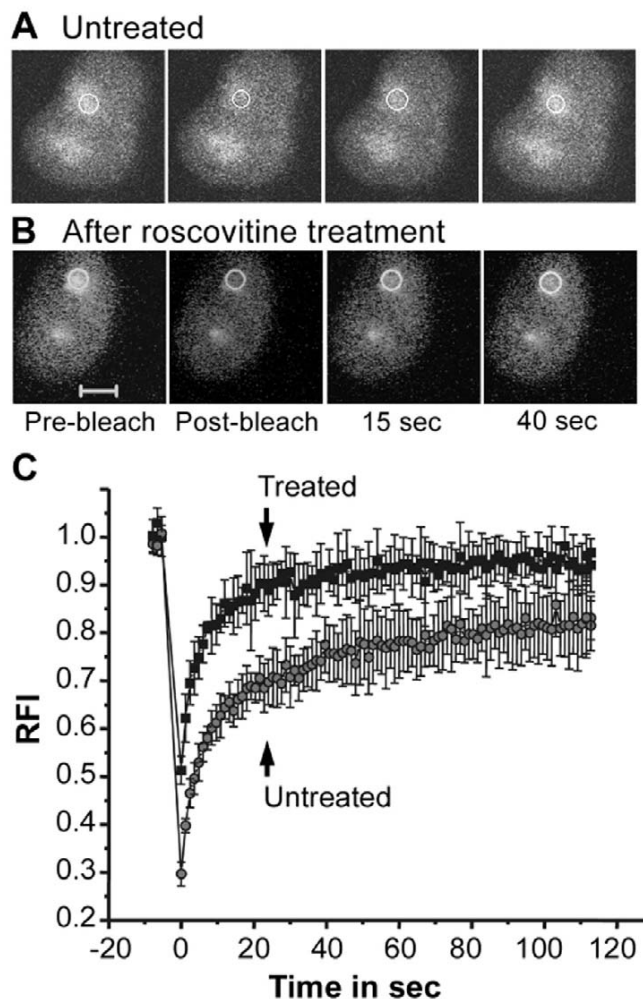


**Figure 5.** Fluorescence recovery after photobleaching (FRAP) analysis of green fluorescent protein (GFP)-fibrillarin. **(A, B)** Fluorescence images of FRAP processes of GFP-fibrillarin in untreated and roscovitine-treated interphase cells. Circles indicate areas of bleaching where fluorescence recovery was measured. Two example time points are shown at 15 and 40 s after photobleaching. Bar, 5  $\mu\text{m}$ . **(C)** Graphical presentation of fluorescence recovery as relative fluorescence intensity (RFI) over time.

#### 4. Discussion

During mitosis, nuclear speckles are disassembled in metaphase and reassembled in telophase as MIGs (Reuter *et al* 1985; Verheijen *et al* 1986; Leser *et al* 1989; Spector *et al* 1991; Ferreira *et al* 1994). We observed that a substantial fraction of GFP-SC35 was localized within telophase nuclei after the formation of the nascent nuclear envelope, while a comparatively smaller amount was present in MIGs. This distribution is distinct from that reported for the splicing factors SF2/ASF or B<sup>7</sup>, which are highly enriched in MIGs in telophase (Prasanth *et al* 2003). The difference in reactivity with a mAb to SC35 suggests

that the SC35 present within telophase nuclei might be in a hypophosphorylated or differentially phosphorylated form compared with the hyperphosphorylated form of SC35 in MIGs. Nuclear speckles are reassembled in G1 nuclei after transient accumulation of splicing factors in patches around active nucleolar organizing regions (NORs) termed NOR-associated patches (NAPs) in telophase nuclei, and a hypophosphorylated form of SC35 has been detected in NAPs (Bubulya *et al* 2004). The different components of the transcription and pre-mRNA splicing machinery show differences in their order of nuclear entry during reformation of the nucleus; based on the observed entry of splicing factors into telophase nuclei with their concomitant reduction in MIGs, it has been suggested that MIGs may serve as recruitment or sites for modification of splicing factors (possibly by phosphorylation) before their migration into telophase nuclei (Prasanth *et al* 2003).

It has been earlier demonstrated that GFP-SF2/ASF rapidly associates with and dissociates from nuclear speckles, and shows similar diffusion coefficients for molecules residing in the nucleoplasm or speckles (Phair and Misteli 2000). In our study, we also obtained similar values for GFP-SC35 in interphase cells. Interestingly, in metaphase cells, GFP-SC35 moves more rapidly than in the interphase nucleoplasm, indicating that its binding interactions in these two compartments are different. Furthermore, our data suggest that the mobility of GFP-SC35 in MIGs is similar to that in interphase speckles or nucleoplasm, in accordance with the view that MIGs are functional counterparts of interphase speckles (Prasanth *et al* 2003). The observed slower mobility of GFP-SC35 in telophase nuclei might be a consequence of the crowded environment of telophase chromatin. The slightly faster mobility of GFP-SC35 in enlarged speckles in interphase cells treated with cdk inhibitors is probably due to the absence of nucleoplasmic binding sites for GFP-SC35 at transcription centres, as roscovitine has been observed to inhibit transcription by inhibiting phosphorylation of the carboxyl-terminal domain of RNA polymerase II (Ljungman and Paulsen 2001). A similar increase in mobility has been reported with GFP-SF2/ASF in cells treated with the transcriptional inhibitor  $\alpha$ -amanitin (Phair and Misteli 2000). In view of the observed phosphorylation of SC35 by Cdk1 *in vitro*, another potential mechanism is that cdk inhibitors might block the phosphorylation of SC35 and thereby hinder its recruitment to transcription sites. This is in accordance with the well documented requirement for phosphorylation of splicing factors to enable their recruitment to transcription sites (Misteli *et al* 1998).

We observed that treatment of cells with roscovitine leads to dispersal of the nucleolar protein fibrillarin in interphase cells, with a concomitant increase in mobility. This increase in mobility may reflect the absence of appropriate binding



sites for fibrillarin after disorganization of the nucleolar compartment due to treatment with roscovitine. Fibrillarin is involved in the processing of rRNA transcripts and interacts with U3 small nucleolar RNA (snoRNA) (Scheer and Hock 1999). Consistent with a requirement for phosphorylation of regulatory factors by cdk2 to increase rDNA transcription (Voit *et al* 1999), treatment with the cdk inhibitor roscovitine causes disorganization of nucleoli (Sirri *et al* 2002).

In summary, the dynamics of splicing factor SC35 depend on the nuclear compartment in which it is localized, particularly in mitotic cells. Furthermore, the mobilities of both GFP-SC35 and GFP-fibrillarin are altered in the presence of a cdk inhibitor in interphase cells. Our results have important implications for understanding how activities of individual components are directed by nuclear compartmentalization.

### Acknowledgements

We thank Tom Maniatis, Sui Huang, Adrian Krainer, L Meijer and David Spector for generous gifts of reagents. We thank Nandini Rangaraj for expert assistance with confocal microscopy and FRAP experiments, and we are grateful to Bh Muralikrishna for help with western blot analysis. Financial support of the Department of Biotechnology, New Delhi for this work is gratefully acknowledged. KT was supported by a pre-doctoral research fellowship from the Council of Scientific and Industrial Research, New Delhi.

### References

- Axelrod D, Koppel D E, Schlessinger J, Elson E and Webb W W 1976 Mobility measurement by analysis of fluorescence photobleaching recovery kinetics; *Biophys. J.* **16** 1055–1069
- Ben-David Y, Lerwin K, Tannock L, Bernstein A and Pawson T 1991 A mammalian protein kinase with potential for serine/threonine and tyrosine phosphorylation is related to cell cycle regulators; *EMBO J.* **10** 317–325
- Bubulya P A, Prasanth K V, Deerinck T J, Gerlich D, Beaudouin J, Ellisman M H, Ellenberg J and Spector D L 2004 SR splicing factors transiently localize around active nucleolar organizing regions in telophase daughter nuclei; *J. Cell Biol.* **167** 1–15
- Carmo-Fonseca M, Pepperkok R, Carvalho M T and Lamond A I 1992 Transcription-dependent colocalization of the U1, U2, U4/U6 and U5 sn-RNPs in coiled bodies; *J. Cell Biol.* **117** 1–14
- Colwill K, Pawson T, Andrews B, Prasad J, Manley J L, Bell J C and Duncan P I 1996 The Clk/Sty protein kinase phosphorylates splicing factors and regulates their intranuclear distribution; *EMBO J.* **15** 265–275
- Fakan S 1994 Perichromatin fibrils are in situ forms of nascent transcripts; *Trends Cell Biol.* **4** 86–90
- Fakan S and Puvion E 1980 The ultrastructural visualization of nucleolar and extranucleolar RNA synthesis and distribution; *Int. Rev. Cytol.* **65** 255–299
- Ferreira J A, Carmo-Fonseca M and Lamond A I 1994 Differential interaction of splicing snRNPs with coiled bodies and interchromatin granules during mitosis and assembly of daughter cell nuclei; *J. Cell Biol.* **126** 11–23
- Fu X-D and Maniatis T 1990 Factor required for mammalian spliceosome assembly is localized to discrete regions in the nucleus; *Nature (London)* **343** 437–441
- Gui J F, Lane W S and Fu X-D 1994 A serine kinase regulates intracellular localization of splicing factors in the cell cycle; *Nature (London)* **369** 678–682
- Herrmann C H and Mancini M A 2001 The Cdk9 and cyclin T subunits of TAK/P-TEFb localize to splicing factor-rich nuclear speckle regions; *J. Cell Sci.* **114** 1491–1503
- Howell B W, Afar D E, Lew J, Douville E M, Icelly P L, Gray D A and Bell J C 1991 STY, a tyrosine-phosphorylating enzyme with sequence homology to serine/threonine kinases; *Mol. Cell Biol.* **11** 568–572
- Johnson K W and Smith K A 1991 Molecular cloning of a novel human cdc2/CDC28-like protein kinase; *J. Biol. Chem.* **266** 3402–3407
- Ko T K, Kelly E and Pines J 2001 CrkRS: a novel conserved Cdc2-related protein kinase that colocalises with SC35 speckles; *J. Cell Sci.* **114** 2591–2603
- Kruhlik M J, Lever M A, Fischle W, Verdin E, Bazett-Jones D P and Hendzel M J 2000 Reduced mobility of the alternate splicing factor (ASF) through the nucleoplasm and steady state speckle compartments; *J. Cell Biol.* **150** 41–51
- Lamond A I and Earnshaw W C 1998 Structure and function in the nucleus; *Science* **280** 547–553
- Lamond A I and Spector D L 2003 Nuclear speckles: a model for nuclear organelles; *Nat. Rev. Mol. Cell Biol.* **4** 605–612
- Leser G P, Fakan S and Martin T E 1989 Ultrastructural distribution of ribonucleoprotein complexes during mitosis. snRNP antigens are contained in mitotic granule clusters; *Eur. J. Cell Biol.* **50** 376–389
- Ljungman M and Paulsen M T 2001 The cyclin-dependent kinase inhibitor roscovitine inhibits RNA synthesis and triggers nuclear accumulation of p53 that is unmodified at Ser15 and Lys382; *Mol. Pharmacol.* **60** 785–789
- Meijer L, Borgne A, Mulner O, Chong J P J, Blow J J, Inagaki N, Inagaki M, Delcros J-G and Moulinoux J-P 1997 Biochemical and cellular effects of roscovitine, a potent and selective inhibitor of the cyclin-dependent kinases cdc2, cdk2 and cdk5; *Eur. J. Biochem.* **243** 527–536
- Mintz P J, Patterson S D, Neuwald A F, Spahr C S and Spector D L 1999 Purification and biochemical characterization of interchromatin granule clusters; *EMBO J.* **18** 4308–4320
- Misteli T, Caceres J F, Clement J Q, Krainer A R, Wilkinson M F and Spector D L 1998 Serine phosphorylation of SR proteins is required for their recruitment to sites of transcription in vivo; *J. Cell Biol.* **143** 297–307
- Misteli T, Caceres J F and Spector D L 1997 The dynamics of a pre-mRNA splicing factor in living cells; *Nature (London)* **387** 523–527
- Misteli T and Spector D L 1999 RNA polymerase II targets pre-mRNA splicing factors to transcription sites in vivo; *Mol. Cell* **3** 697–705
- Phair R D and Misteli T 2000 High mobility of proteins in the mammalian cell nucleus; *Nature (London)* **404** 604–609

- Politz J C R, Tuft R A, Prasanth K V, Baudendistel N, Fogarty K E, Lifshitz L M, Langowski J, Spector D L and Pederson T 2006 Rapid, diffusional shuttling of poly(A) RNA between nuclear speckles and the nucleoplasm; *Mol. Biol. Cell* **17** 1239–1249
- Prasanth K V, Sacco-Bubulya P A, Prasanth S G and Spector D L 2003 Sequential entry of components of gene expression machinery into daughter nuclei; *Mol. Biol. Cell* **14** 1043–1057
- Reuter R, Appel B, Rinke J and Luhrmann R 1985 Localization and structure of snRNPs during mitosis. Immunofluorescent and biochemical studies; *Exp. Cell Res.* **159** 63–79
- Sacco-Bubulya P and Spector D L 2002 Disassembly of interchromatin granule clusters alters the coordination of transcription and pre-mRNA splicing; *J. Cell Biol.* **156** 425–436
- Scheer U and Hock R 1999 Structure and function of the nucleolus; *Curr. Opin. Cell Biol.* **11** 385–390
- Sirri V, Hernandez-Verdun D and Roussel P 2002 Cyclin-dependent kinases govern formation and maintenance of the nucleolus; *J. Cell Biol.* **156** 969–981
- Spector D L 1993 Macromolecular domains within the cell nucleus; *Annu. Rev. Cell Biol.* **9** 265–315
- Spector D L 2003 The dynamics of chromosome organisation and gene regulation; *Ann. Rev. Biochem.* **72** 573–608
- Spector D L, Fu X-D and Maniatis T 1991 Associations between distinct pre-mRNA splicing components and the cell nucleus; *EMBO J.* **10** 3467–3481
- Verheijen R, Kuijpers H, Voojjs P, van Venrooij W and Ramaekers F 1986 Protein composition of nuclear matrix preparations from HeLa cells: an immunochemical approach; *J. Cell Sci.* **80** 103–122
- Voit R, Hoffmann M and Grummt I 1999 Phosphorylation by G1-specific cdk–cyclin complexes activates the nucleolar transcription factor UBF; *EMBO J.* **18** 1891–1899

*MS received 20 November 2007; accepted 23 May 2008*

ePublication: 28 June 2008

Corresponding editor: VIDYANAND NANJUNDIAH